Firstly it must be possible from the ordinary data available at the structure refinement stage (*viz* cell dimensions and space group) to generate the possible twinning operations due to (pseudo-)merohedry. One of the algorithms described in this paper can be used for this purpose. The second ingredient is the capability to refine the volume fractions of the twin components as variables in the least squares. In principle this poses no major difficulties although attention should be paid to such questions as scale-factor refinement, intensity-data structuring, evaluation of Fourier coefficients for electron density calculation and rotation and/or inversion of atomic parameters. These questions will be examined in detail in a future publication. The treatment of twinning resolves not only the problem of twinned crystals but also solves the difficulties of orientation ambiguities when working from a known list of atomic positional parameters. As an illustration, in the refinements of Nb_3Si and Nb_3As undertaken by Waterstrat, Yvon, Flack & Parthé (1975) from published atomic parameters (see second example above), one compound refined immediately to a low R value whilst the second remained at 50%. When the reflection indices were transformed by the above twin law, the R value of the second compound diminished immediately to a low value. An automatic twin-component refinement would have saved some considerable anxiety and immediately resolved this orientation ambiguity.

The problems of twinning and space-group ambiguities with disorder are intimately related. The coset decomposition of the metric symmetry with respect to the crystal point group furnishes the rotation matrices necessary to describe the merohedral twin laws. It is of course possible in practice that, instead of twinning, disorder could arise and that the declared space group is a subgroup of the correct one. The coset decomposition produces the rotational components of the 'missing' symmetry operations. It would remain to find the translational parts by some other technique.

The author wishes to thank Dr Y. Le Page and Dr W. Depmeier for very helpful criticism on a first draft of this paper.

References

Bernardinelli, G. & Flack, H. D. (1985). *Acta Cryst.* **A41**, 500-511.
Bernardinelli, G. & Flack, H. D. (1987). *Acta Cryst.* **A43**, 75-78.
Flack, H. D. (1983). *Acta Cryst.* **A39**, 876-881.
International Tables for Crystallography (1983). Vol. A. Dordrecht: Reidel.
Klee, W. E. & Wondratschek, H. (1984). *Elements of Crystallography. Course Notes of the International Summer School on Symmetry-Related Crystal Structures; Group-Subgroup Relations.* Rauischholzhausen, Federal Republic of Germany.
Le Page, Y. (1982). *J. Appl. Cryst.* **15**, 255-259.
Le Page, Y., Donnay, J. D. H. & Donnay, G. (1984). *Acta Cryst.* **A40**, 679-684.
Stewart, J. M., Machin, P. A., Dickinson, C. W., Ammon, H. L., Heck, H. & Flack, H. (1976). The *XRAY*76 system. Tech. Rep. TR-446. Computer Science Center, Univ. of Maryland, College Park, Maryland, USA.
Waterstrat, R. M., Yvon, K., Flack, H. D. & Parthé, E. (1975). *Acta Cryst.* **B31**, 2765-2769.
Zimmermann, H. & Burzlaff, H. (1985). *Z. Kristallogr.* **170**, 241-246.

Acta Cryst. (1987). **A43**, 568-572

The Visibility of Phase Indications in *n*-Beam Diffraction Patterns*

By Ben Post and Walter Kiszenick

Physics Department, Polytechnic University, 333 *Jay Street, Brooklyn, NY* 11201, *USA*

(*Received* 9 *December* 1986; *accepted* 23 *February* 1987)

Abstract

[0*k*0] *n*-beam diffraction patterns of germanium have been recorded by rotation of specimens about the diffraction vectors of the vanishingly weak 020 and 060, and the very strong 040 reflections. *N*-beam interactions were displayed clearly in the [020] and [060] scans, and somewhat less clearly in the [040] scan. Unambiguous phase indications, however, were detected only in the [040] scan. The experiments demonstrate that the visibility of *n*-beam *interactions* does not necessarily imply a corresponding visibility of experimental *phase indications*. The geometry of some unusual four- and five-beam interactions detected in the [0*k*0] scans, and the phases shown by those interactions, are also discussed.

I. Introduction

The visibility of *n*-beam interactions in Renninger patterns increases monotonically with decreasing two-beam background intensity, *i.e.* with decreasing intensity of the primary reflection. It is therefore often assumed that only weak primary reflections are suited

* Work supported by the Division of Materials Research of the National Science Foundation, Grant DMR 8311525, and in part by the Joint Services Electronics Program, Contract no. F49620-82-C-0084.

0108-7673/87/040568-05$01.50

for use in experimental investigations of X-ray reflection phases (Han & Chang, 1983). Very few reasonably complete sets of experimental n-beam data dealing with the determination of reflection phases are available in the published literature to provide definitive checks on the validity of that assumption. A sampling of the few that are available may be of some use for that purpose.

The phase indications displayed in an n-beam pattern of germanium, recorded by rotation of the crystal about the diffraction vector of the 'forbidden' 222 reflection, have been discussed by Post, Nicolosi & Ladell (1984). Although many of the phase indications were weak, it was possible to determine 15 of the 17 triplet phases in the asymmetric 30° range of the pattern.

Very strong phase indications were observed in [040] n-beam patterns of monoclinic crystals of $ZnWO_4$ (Gong & Post, 1983). In that case, the primary reflection was relatively intense. The magnitude of its structure factor equalled 62, compared with 150 for the strongest $ZnWO_4$ reflection.

Strong phase indications have also been observed by Post, Gong, Kern & Ladell (1986) in [311] n-beam patterns of germanium. The structure factor of the 311 reflection is approximately two-thirds as large as that of the strongest germanium reflection, 220. Nevertheless, all the calculated n-beam interactions were detected in the Renninger pattern. The triplet phases of all the interactions, except for those which included 'forbidden' reflections, were determined. More recently, Post & Ladell (1987) used additional [311] data to determine the phases of many of the weak interactions; each of the latter included one forbidden reflection.

Additional data are needed, but it is clear from the above that it is not necessary to limit the choice of primary reflections to weak reflections in experimental phase investigations.

The objectives of this work include detailed comparisons of the phase indications displayed in Renninger patterns recorded with very strong and very weak primary reflections. The $0k0$ reflections of germanium are well suited for that purpose. Only three $0k0$ reflections are accessible to the Cu $K\alpha_1$ radiation used in this work: 020, 040 and 060. The 020 and 060 reflections are 'forbidden' in diamond-type crystals; 040 is one of the strongest germanium reflections.

Some unusual n-beam interactions, detected in the [$0k0$] patterns, and the possibility of extracting phase information from such interactions, will also be discussed below.

II. Experimental

The experimental arrangement used by Gong & Post (1983) has been modified slightly for use in this investigation. The X-ray source was a $0{\cdot}3\times 3$ mm copper target of a Rigaku–Denki rotating-anode generator. To reduce the divergence of the incident beam, a 2 m long evacuated pipe was placed between the X-ray source and the specimen. A 6° take-off angle reduced the effective size of the target to $0{\cdot}3\times 0{\cdot}3$ mm. Passage of the incident beam through a 0·3 mm pinhole near the specimen limited its divergence to less than a minute of arc.

Disks of etched and polished germanium, cut perpendicular to [$0k0$], were used as specimens. The crystals were rotated about [$0k0$] at a rate of $0{\cdot}25°\,\mathrm{min}^{-1}$. Diffracted intensities were recorded with a scintillation detector which remained fixed at the appropriate 2θ setting throughout each experiment.

Additional details concerning experimental arrangements and procedures for extracting phases from the experimental data are given in Gong & Post (1983) and Post, Nicolosi & Ladell (1984).

III. Experimental results and discussion

A. General considerations

Reflections whose indices sum to $4n\pm 2$ are 'forbidden' in diamond-type crystals. Their structure factors equal zero when they are calculated according to the extinction rules for spherically symmetric atoms in positions $8a$ of space group $Fd3m$, as listed in *International Tables for X-ray Crystallography* (1952).

It is useful to divide such forbidden reflections into two categories: those whose indices include one or two zeros, and those in which all the indices differ from zero. The former, *e.g.* 020 and 420, have been labelled 'strictly fobidden' by Dawson (1967); their calculated structure factors equal zero when effects due to an anomalous dispersion are not included in the calculations (Dawson, 1967; Willis & Pryor, 1975). The contributions of anomalous scattering to diffraction by those reflections are finite, but extremely weak. We are not aware of any reliable reports of detection of experimental two-beam 020 or 060 intensities diffracted by diamond-type crystals.

Measurements of the intensities of reflections in the second category, such as 222, 442 and 622, show that they differ from zero by small amounts, due mainly to anharmonic thermal motions and distortions of the bonding electron distributions. In those reflections the differences from zero persist even when effects due to anomalous dispersion have been removed from the measured intensities (Trucano & Batterman, 1972; Hastings & Batterman, 1975; Tischler & Batterman, 1984).

B. [$0k0$] *n-beam patterns*

Renninger scans recorded by rotation about [020], [040] and [060] are shown in Figs. 1–3. Each chart displays the asymmetric range of 45°. A 12° region

Table 1. *Data for the* [020] *n-beam pattern of germanium with* Cu $K\alpha_1$ *radiation* ($\lambda = 1{\cdot}5406$ Å)

No.	RLP			COUPLE			E/L	BETA
1	−3	−1	−3	3	3	3	0·545	−91·09
2	−1	1	−7	1	1	7	3·205	−22·67
3	3	3	−5	−3	−1	5	4·839	52·25
4	3	1	−1	−3	1	1	5·312	132·506
5	−3	1	−5	3	1	5	5·832	−73·592
6	−3	1	−3	3	1	3	10·462	−110·924
7	−1	−1	−1	1	3	1	14·983	−119·966
8	3	3	−1	−3	−1	1	17·133	108·864
9	1	1	−7	−1	1	7	19·465	−22·67
10	5	1	−3	−5	1	3	22·24	73·592
11	−1	3	−5	1	−1	5	25·107	−72·834
12	5	1	−1	−5	1	1	32·616	92·148
13	5	−1	−3	−5	3	3	32·911	52·25
14	5	1	−5	−5	1	5	33·665	22·67
15	−1	1	−5	1	1	5	34·764	−92·148
16	−1	−1	−3	1	3	3	35·997	−108·864
17	−1	1	−1	1	1	1	39·258	−168·516
18	3	1	1	−3	1	−1	42·182	132·506
19	5	−1	−1	−5	3	1	42·273	72·834

Table 2. *Data for the* [040] *n-beam pattern of germanium with* Cu $K\alpha_1$ *radiation* ($\lambda = 1{\cdot}5406$ Å)

No.	RLP			COUPLE			E/L	BETA
1	2	2	0	−2	2	0	0	180
2	3	3	−5	−3	1	5	0·621	60·686
3	1	−1	−5	−1	5	5	2·024	18·572
4	3	1	−1	−3	3	1	2·624	137·882
5	1	5	−1	−1	−1	1	8·464	73·072
6	4	2	−2	−4	2	2	8·939	108·992
7	−3	1	−3	3	3	3	9·976	−109·952
8	3	−1	−3	−3	5	3	16·644	56·712
9	−2	4	−2	2	0	2	17·669	−125·338
10	1	5	−5	−1	−1	5	20·596	−18·572
11	−1	5	−3	1	−1	3	21·212	−79·294
12	4	4	−4	−4	0	4	21·675	46·65
13	−2	2	−4	2	2	4	27·931	−108·992
14	5	1	−3	−5	3	3	28·693	60·686
15	0	2	−6	0	2	6	30·031	−60·062
16	−1	1	−5	1	3	5	31·618	−85·856
17	3	5	−1	−3	−1	1	31·918	79·294
18	5	1	−1	−5	3	1	35·762	85·856
19	1	3	1	−1	1	−1	38·409	193·182
20	3	1	1	−3	3	−1	39·494	137·882
21	4	0	0	−4	4	0	40·49	99·02

within which no interactions were detected has been omitted from Fig. 3. Relevant data for each chart are listed in Tables 1-3. The numbers listed next to the maxima in Figs. 1 and 3 correspond to those in column 1 of the tables. They identify the *n*-beam interactions. The indices of reciprocal-lattice points (r.l.p.s) which generate *n*-beam interactions when they cross the surface of the Ewald sphere, *i.e.* the 'transit' r.l.p.s, are listed under 'RLP'; the indices of the coupling terms are given in the adjacent column. The angle settings at which transit r.l.p.s enter or leave the sphere appear under 'E/L'. The angular separations between the settings at which a given r.l.p. enters and leaves the sphere are listed under 'BETA'. A negative number indicates that the corresponding entry in the 'E/L' column refers to a r.l.p. which is leaving the sphere To save space, only one 'transit' and one 'coupling' term are listed for each interaction. Two such sets are involved in each four-beam interaction.

Diffraction profile asymmetries, from which triplet or quartet phases can be deduced, are readily detected in Fig. 2. Five interactions which display the clearest phase indications are shown in Fig. 4. 'Entering' and 'leaving' interactions are shown side by side. To record the Fig. 4 interactions, the azimuthal rotation speed of the crystal was reduced by a factor of two relative to that used for the Fig. 2 scan.

It has been shown (Post, Gong, Kern & Ladell, 1986) that the calculated phases of all germanium triplets and quartets are positive, except for those which include forbidden reflections. No forbidden reflections are present in the interactions shown in Fig. 4. All the latter therefore display identical intensity sequences which indicate positive phases, *i.e.* attenuation followed by enhancement, on entering the sphere, and the reverse sequence on leaving. The 'entering' direction in Figs. 1-4 is from right to left.

No unambiguous phase indications comparable to those shown in Fig. 4 were detected in Figs. 1 or 3. Faint indications of possible profile asymmetries were detected in a few interactions. Repeated scans at

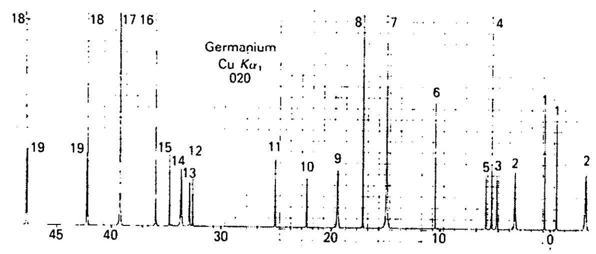

Fig. 1. [020] *n*-beam pattern of germanium (Cu $K\alpha_1$ radiation).

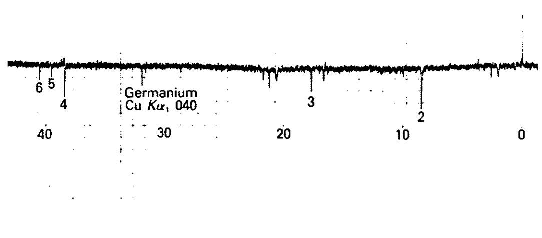

Fig. 2. [040] *n*-beam pattern of germanium (Cu $K\alpha_1$ radiation).

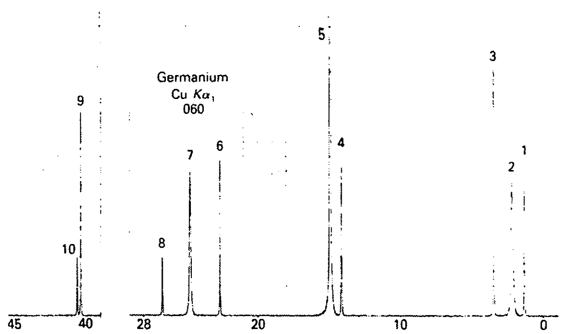

Fig. 3. [060] *n*-beam pattern of germanium (Cu $K\alpha_1$ radiation).

Table 3. *Data for the* [060] *n-beam pattern of germanium with* Cu $K\alpha_1$ *radiation* ($\lambda = 1{\cdot}5406$ Å)

No.	RLP			COUPLE			E/L	BETA
1	3	1	−3	−3	5	3	1·322	87·356
2	−1	5	−5	1	1	5	2·26	−27·14
3	3	5	−1	−3	1	1	3·478	136·174
4	−3	3	−1	3	3	1	14·154	−171·438
5	−3	3	−3	3	3	3	14·954	−119·908
6	3	3	1	−3	3	−1	22·716	171·438
7	1	5	−5	−1	1	5	24·88	−27·14
8	−1	3	−5	1	3	5	26·791	−76·202
9	3	1	1	−3	5	−1	40·348	136·174
10	5	3	−1	−5	3	1	40·589	76·202

varying speeds, some as slow as 0·6° h^{-1}, showed that the 'asymmetries', with the possible exception of the one shown by no. 5 of Fig. 3, were not reproducible. We were unable to establish whether the latter was due to a very weak phase indication or to some unidentified artifacts. In any event, it is clear that the factors which determine the visibility of *maxima* in n-beam interactions are not necessarily the same as those which determine the visibility of *phase indications.*

C. *Four-beam interactions*

The four r.l.p.s involved in each four-beam [$0k0$] interaction are located at the corners of symmetrical trapezoids (Fig. 5). Squares and rectangles are special cases of such trapezoids. In each interaction the rotation axis is involved in two triplets. The trapezoids may be described in terms of their two parallel sides, *i.e.* [020]/[040], [040]/[060] and [020]/[060]. Either side may serve as the rotation axis. N-beam maxima due to the first two types are detected in the [$0k0$] patterns; those due to the third type, [020]/[060], are not.

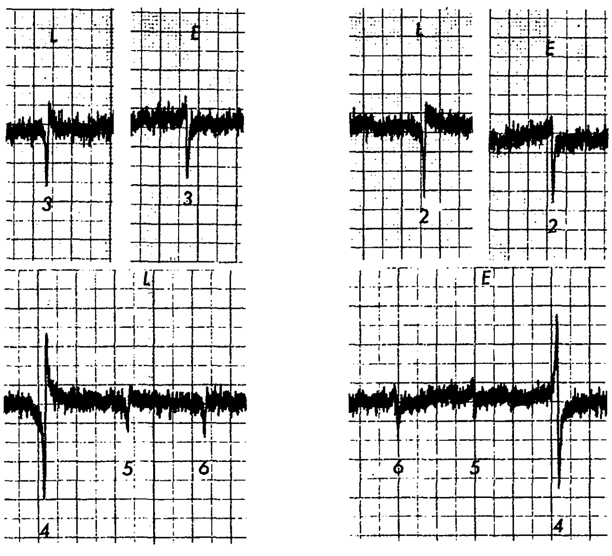

Fig. 4. Selected [040] interactions: 'E'=entering; 'L'=leaving.

The sums of the phases of reflections whose diffraction vectors form closed polygons in reciprocal space are 'invariant'. [$0k0$] triplets composed of three even-index terms each of which sums to $4n$, or of one even-index and two odd-index terms, are also invariant and are usually detectable. Even-index triplets may also consist of two terms, each of which sums to $4n \pm 2$, and one which sums to $4n$. Such triplets include two forbidden reflections (see Fig. 5). They are extremely weak and are generally not observed. The [020]/[060] trapezoids generate such triplets and are therefore not detected.

A four-beam interaction, involving (000), (040), (220), (2$\bar{2}$0), is listed as no. 1 in Fig. 2. The four r.l.p.s are located at the corners of the square shown in Fig. 6. Rotation about [040] can bring the plane of the r.l.p.s to settings perpendicular to a line from the center of the sphere. R.l.p.s 2, 2, 0 and 2, −2, 0, as well as 0, 0, 0 and 0, 4, 0, then lie on the circular intersection of the plane shown in Fig. 6 and the Ewald sphere. The four r.l.p.s diffract simultaneously.

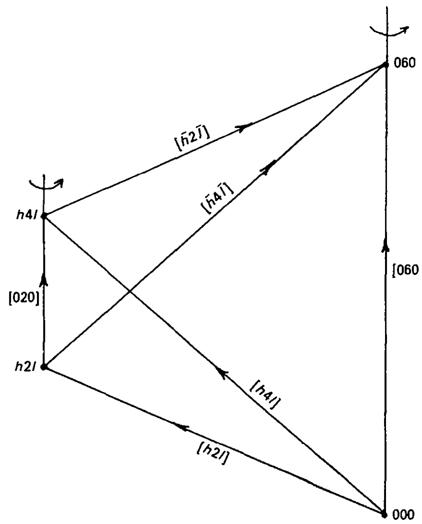

Fig. 5. A symmetrical four-beam interaction; r.l.p.s at the corners of a symmetrical trapezoid.

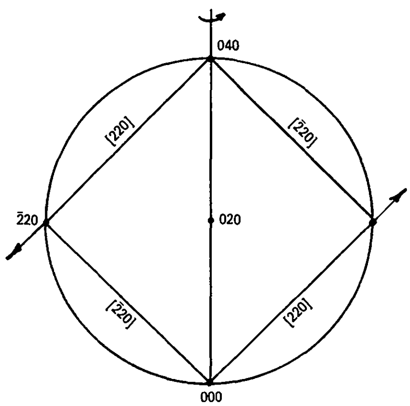

Fig. 6. Arrangement of r.l.p.s in the four-beam (000), (040), (220), ($\bar{2}$20) interaction.

R.l.p.s 2, 2, 0 and 2, −2, 0, however, move in opposite directions. One enters the sphere while the other is leaving. That four-beam interaction may therefore be viewed as two opposed simultaneous three-beam interactions. The superposition of the two equal and opposite phase effects leads to cancellation of the phase indications. The intensities of the interactions would vanish if the overall enhancement above the two-beam background were equal in magnitude to the attenuation below that background. Similar partial or complete cancellations of phase indications and intensities occur in all cases in which the rotation axis is a diagonal of a four-beam or higher-order polygon.

D. *Interesting five-beam interactions*

The arrangements and indices of the r.l.p.s involved in strong five-beam interactions detected in [040] and [060] scans (no. 2 in Figs. 2 and 4, and no. 5 in Fig. 3) are illustrated in Figs. 7(*a*) and (*b*). Broken lines in the figures indicate that the corresponding reflections are forbidden. The r.l.p.s are located at the corners of symmetrical pentagons. Although the indices of the r.l.p.s in Figs. 7(*a*) and (*b*) differ, both figures represent the same pentagon. The differences between the two sets of indices reflect the change of origin in going from Fig. 7(*a*) to Fig. 7(*b*).

In Fig. 7(*a*), the rotation axis, [060], is a diagonal of the pentagon. As indicated above, rotation about that axis causes two r.l.p.s, −1, 1, 1 and −1, 5, 1, to enter the Ewald sphere while 3, 3, −3 is leaving, or the reverse. In Fig. 7(*b*) the [040] rotation axis is one of the sides of the pentagon. Three r.l.p.s then enter and leave the sphere simultaneously when the crystal is rotated.

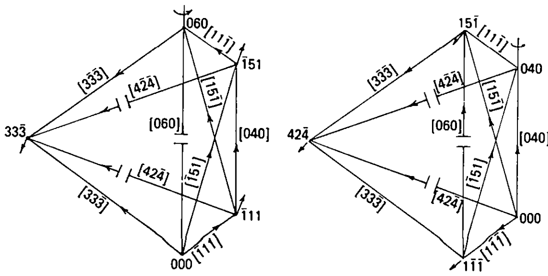

(*a*) (*b*)

Fig. 7. A five-beam interaction: (*a*) in the [060] scan; (*b*) in the [040] scan.

The invariant phase of Fig. 7(*b*) is displayed clearly in interaction no. 2 of Figs. 2 and 4. The indicated phase is positive, consistent with the assumption that the experimental five-beam phase is determined by the triplets in which the rotation axis is involved: (040), ($1\bar{1}\bar{1}$), ($15\bar{1}$) and (040), ($11\bar{1}$), ($\bar{1}5\bar{1}$). A third triplet (040), ($4\bar{2}\bar{4}$), ($42\bar{4}$) is not considered because two of its components represent forbidden reflections. No comparable, unambiguous phase indication is shown by the Fig. 7(*a*) interaction.

Five-beam interactions, such as the one shown in Fig. 7, can be generated in each of the ten *n*-beam scans in which one of the ten vectors (five sides and five diagonals) serves as the rotation axis. These could provide a number of opportunities to check on the validity of the assumption noted above, *i.e.* that the experimental five-beam phases, like their four-beam counterparts, are determined by the triplets in which the rotation axes are involved.

IV. Summary

The experimental evidence given above indicates that the use of weak primary reflections in *n*-beam investigations to improve the visibility of Renninger interactions does not necessarily lead to improved visibility of *n*-beam phase indications. Visibility of interactions is a necessary but not sufficient condition for detectable phase indications.

The important part played by triplets in which the rotation axis is involved, in determining experimental phase indications, is shown to hold for five- as well as four-beam cases.

References

Dawson, B. (1967). *Proc. R. Soc. London Ser. A*, **298**, 304–313.
Gong, P. P. & Post, B. (1983). *Acta Cryst.* **A39**, 719–724.
Han, F. S. & Chang, S. L. (1983). *Acta Cryst.* **A39**, 98–101.
Hastings, J. B. & Batterman, B. W. (1975). *Phys. Rev. B*, **12**, 5580–5584.
International Tables for X-ray Crystallography (1952). Vol. I, p. 341. Birmingham: Kynoch Press.
Post, B., Gong, P. P., Kern, L. & Ladell, J. (1986). *Acta Cryst.* **A42**, 178–184.
Post, B. & Ladell, J. (1987). *Acta Cryst.* **A43**, 173–179.
Post, B., Nicolosi, J. & Ladell, J. (1984). *Acta Cryst.* **A40**, 684–688.
Tischler, J. Z. & Batterman, B. W. (1984). *Phys. Rev. B*, **30**, 7060–7066.
Trucano, P. & Batterman, B. W. (1972). *Phys. Rev. B*, **6**(10), 3654–3666.
Willis, B. T. M. & Pryor, A. W. (1975). *Thermal Vibrations in Crystallography*, Ch. 5. Cambridge Univ. Press.